Available online at www.sciencedirect.com

SciVerse ScienceDirect

Ceramics International 39 (2013) 725–730

CERAMICS INTERNATIONAL

www.elsevier.com/locate/ceramint

Phase transition behavior and electrical properties of lead-free $(Bi_{0.5}K_{0.5})TiO_3$–$LiNbO_3$ relaxor ferroelectric ceramics

Wenwu Zuo, Ruzhong Zuo*, Wanli Zhao

Institute of Electro Ceramics and Devices, School of Materials Science and Engineering, Hefei University of Technology, Hefei 230009, PR China

Received 19 May 2012; received in revised form 26 June 2012; accepted 26 June 2012
Available online 1 July 2012

Abstract

$(1-x)(Bi_{0.5}K_{0.5})TiO_3$–$xLiNbO_3$ ($(1-x)$BKT–xLN) lead-free relaxor ferroelectric ceramics were prepared by a conventional solid-state route and their phase transition behavior and the corresponding electrical properties were investigated. A morphotropic phase boundary separating rhombohedral and tetragonal phases was identified in the composition range of $0.015 < x < 0.03$, where the improved electrical properties of piezoelectric constant $d_{33}=75$ pC/N and electromechanical coupling factor $k_p=0.18$ were obtained. Moreover, all samples show typical relaxor behavior characterized by the presence of diffuse phase transition and frequency dispersion. It was found that the dielectric relaxation behavior of BKT ceramics can be obviously enhanced with the addition of LN. In addition, the effect of the LN addition on the ferroelectric properties was also investigated by measuring polarization versus electric field hysteresis loops.
© 2012 Elsevier Ltd and Techna Group S.r.l. All rights reserved.

Keywords: $(Bi_{0.5}K_{0.5})TiO_3$; $LiNbO_3$; Phase transition; Relaxor ferroelectric ceramics

1. Introduction

Lead-free piezoelectric ceramics have attracted considerable attention in recent years because of the concerns of the environment pollution and human health. (Na, K)NbO_3 (NKN) is one of lead-free ferroelectric materials that have been widely investigated during the last years owing to their relative high Curie temperatures (T_c) and moderate piezoelectric response [1]. However, the electrical properties of NKN based materials show distinct processing sensitivity and temperature instability probably induced by the existence of polymorphic phase transition [2]. As well known, one of the most effective approaches to obtain high piezoelectric activity is to form ferroelectric solid solutions with a morphotropic phase boundary (MPB) that separates rhombohedral symmetry from tetragonal symmetry. The increase of the dielectric, piezoelectric and electromechanical properties near MPB was attributed to the coexistence of tetragonal and rhombohedral symmetries. Therefore, there has been increasing interest in MPB lead-free ferroelectric systems. Unfortunately, these attempts have been limited by the lack of lead-free end members with higher tetragonality and T_c.

$(Bi_{0.5}K_{0.5})TiO_3$ (BKT) and $Bi(Zn_{0.5}Ti_{0.5})O_3$ (BZT) have been considered as two main lead-free tetragonal perovskite ferroelectrics with relative high T_c values. However, it is found that BZT exhibits very low structural stability under atmospheric conditions [3]. By comparison, BKT is a promising ferroelectric material with a stable perovskite structure, exhibiting a relatively high T_c in the range 380–420 °C. In addition, it also shows distinct relaxor behavior, characterized by the broad dielectric constant maxima as well as frequency dispersion [4]. In perovskite-structured materials, the relaxor behavior was usually seen in lead-based compositions, such as $Pb(Mg_{1/3}Nb_{2/3})O_3$ [5], $Pb(Sc_{1/2}Nb_{1/2})O_3$ [6] and $(Pb,La)(Zr,Ti)O_3$ [7]. These relaxor ferroelectric materials show excellent dielectric and electromechanical properties. It should be also of interest to prepare BKT-based relaxor ferroelectrics and investigate their phase structure and electrical properties. Only a few

*Corresponding author. Tel./fax: +86 551 2905285.
E-mail address: piezolab@hfut.edu.cn (R. Zuo).

0272-8842/$36.00 © 2012 Elsevier Ltd and Techna Group S.r.l. All rights reserved.
http://dx.doi.org/10.1016/j.ceramint.2012.06.084

BKT-based solid solutions have been so far reported [8–10], compared to the widely studied NKN based or $(Bi_{0.5}Na_{0.5})TiO_3$-based materials.

$LiNbO_3$ (LN) has an ilmenite structure, which can be described as a heavily distorted perovskite [11]. As a small amount of LN was added into NKN, the phase structure transformation from orthorhombic to tetragonal structures was induced [12]. It is thus expected that a phase structure change in BKT can be triggered by adding a small amount of LN. In addition, the addition of LN might also enhance the relaxor behavior of BKT, which is similar to some other perovskite ferroelectric materials [13,14].

For the above purposes, $(1-x)$BKT–xLN lead-free ceramics were prepared in this study via a conventional solid-state method and the effect of the substitution of LN for BKT on the dielectric relaxor behavior, phase transition behavior, and ferroelectric and piezoelectric properties was investigated in detail.

2. Experimental

$(1-x)$BKT–xLN ceramics ($x=0$, 0.015, 0.03, 0.06 and 0.09) were prepared by a conventional solid-state reaction method using Bi_2O_3, TiO_2, Li_2CO_3, K_2CO_3 and Nb_2O_5 as starting powders. After weighing, the powders were mixed for 4 h and then calcined at 950 °C for 3 h in air. After the powders were ball-milled again, pellets of 10 mm in diameter and 1 mm in thickness were uniaxially pressed. Sintering was carried out in air at 1000–1100 °C for 3 h.

The room-temperature crystal structures of all specimens were examined by an X-ray diffractometer (XRD, D/MAX2500VL/PC, Rigaku, Japan). After silver paste was fired on major surfaces at 550 °C for 30 min as the electrodes, the dielectric properties of unpoled samples sintered at optimal temperatures were measured as function of temperature and frequency by means of an LCR meter (E4980A, Agilent, Santa Clara, CA). Polarization versus electric field (P–E) hysteresis loops were measured using a ferroelectric measuring system (Precision LC, Radiant Technologies Inc., Albuquerque, NM). The samples were poled in silicone oil at 120 °C under an electric field of 3 kV/mm for 15 min. The piezoelectric strain constant d_{33} of poled samples was measured by a Belincourt-meter (YE2703A, sinocera, Yangzhou, China).

3. Results and discussion

Fig. 1 shows the XRD patterns at room temperature for the $(1-x)$BKT–xLN ceramics with various x values. It was found that most compositions exhibit a single perovskite structure and only a trace of the secondary phase can be detected as the LN content x is higher than 0.09. The possible reason could be ascribed to different crystal structures between BKT (perovskite structure) and LN (ilmenite structure). As $x=0.09$, the solubility limit of LN in the BKT lattice was reached. Moreover, it is worthy to

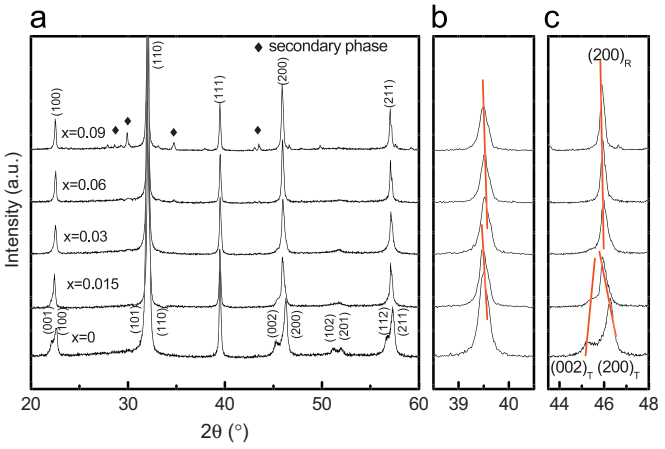

Fig. 1. (a) XRD patterns of $(1-x)$BKT–xLN solid solution ceramics, and locally magnified patterns of (b) (111) and (c) (200) reflection lines.

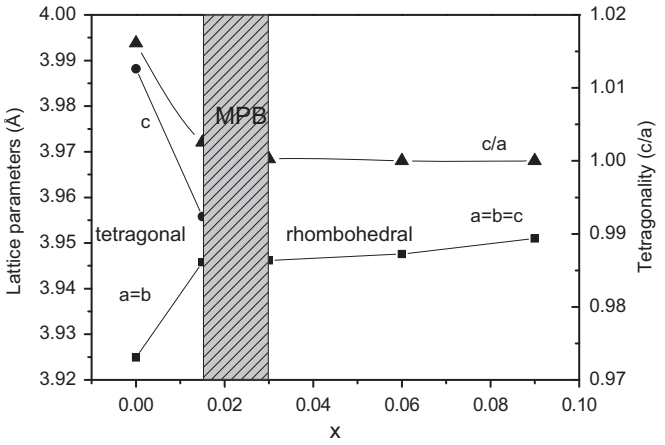

Fig. 2. Lattice parameters of $(1-x)$BKT–xLN ceramics as a function of the LN content.

note that the addition of LN tends to change the crystal symmetry of BKT samples. It was known that pure BKT has a tetragonal symmetry with a small tetragonality (c/a=1.016) [15], as characterized by the splitting of (200) and (002) diffraction peaks. Owing to the addition of LN, the (200) and (002) diffraction peaks merge gradually into a single one, meaning that the phase structure changes from tetragonal to rhombohedral symmetries, which can be clearly seen from the {200} reflection lines given in Fig. 1(c). Therefore, an MPB that separates tetragonal from rhombohedral phases can be identified in the composition range of $0.015<x<0.03$. In addition, it could be seen from Fig. 1(b) that the diffraction peaks shift to lower diffraction angles with increasing the LN content. However, the peak shifts to the higher diffraction angles abruptly when x reaches 0.03. This discontinuous change of the diffraction peak positions can further confirm the appearance of the phase transition. In order to investigate the phase structure change in more details, the lattice parameters of $(1-x)$BKT–xLN ceramics were calculated by fitting the diffraction peak profiles, as shown in Fig. 2.

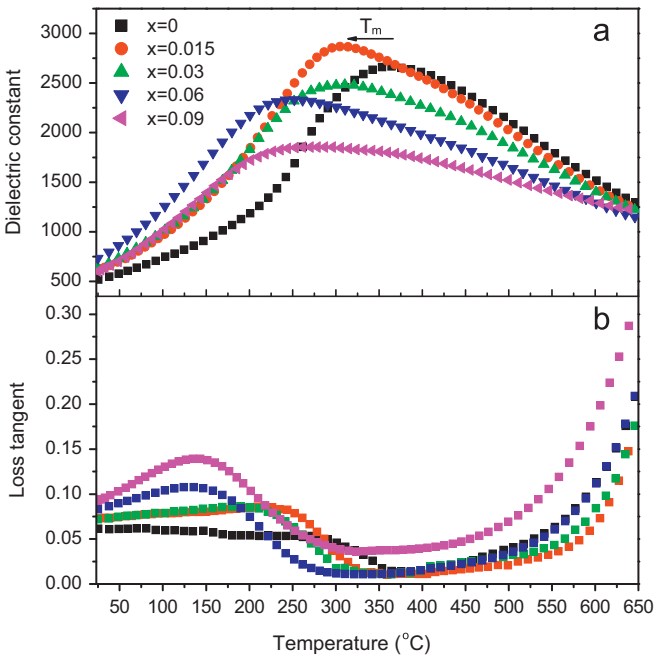

Fig. 3. Dielectric constant (a) and loss tangent (b) at 100 kHz versus temperature curves for $(1-x)$BKT–xLN ceramics as indicated.

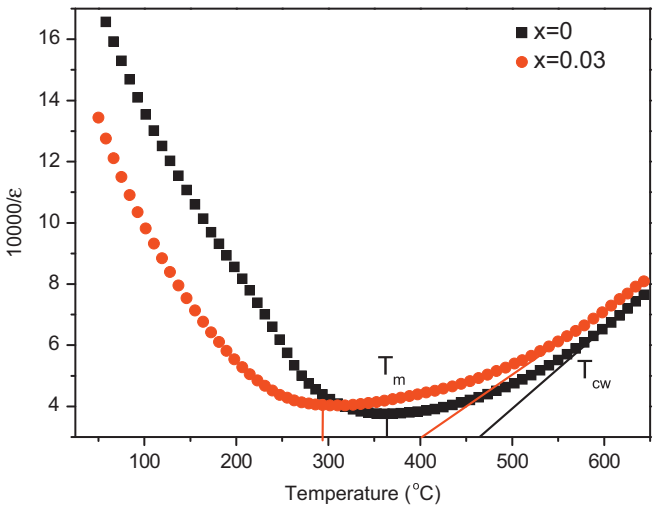

Fig. 4. Plots of the inverse dielectric constant at 100 kHz as a function of temperature for $(1-x)$BKT–xLN ceramics as indicated.

It can be seen that the tetragonality of the compositions decreases rapidly with the addition of LN. A complete rhombohedral symmetry can be found as x is larger than 0.03.

The dielectric constant ε_r and loss tangent at 100 kHz of $(1-x)$BKT–xLN ceramics as a function of temperature are shown in Fig. 3. The temperature T_m at the maximum dielectric constant obviously decreases with the addition of LN. The T_m value is approximately 306 °C for the composition with $x=0.015$. It decreases rapidly to 246 °C for the composition with $x=0.09$. Nevertheless, these T_m values are still much higher than room temperature within the studied composition range. This further indicates that the samples with higher LN content are ferroelectric rhombohedral phases rather than paraelectric cubic phases. In particular, all samples show distinct characteristics of the diffuse phase transition with broad dielectric peaks. With increasing the LN content, the dielectric peak near T_m becomes broader and shifts to lower temperatures.

For normal ferroelectrics, the dielectric constant above the Curie temperature follows the Curie–Weiss law described by [16]

$$1/\varepsilon = (T-T_o)/C (T > T_C) \quad (1)$$

where T_o is the Curie–Weiss temperature and C is the Curie-Weiss constant. However, it is found that the dielectric constant of $(1-x)$BKT–xLN ceramics shows obvious deviation from the Curie–Weiss law. Fig. 4 shows the plots of the inverse dielectric constant versus temperature at 100 kHz for the $x=0$ and $x=0.03$ samples. The parameter ΔT_m, which describes the deviation degree from the Curie–Weiss law, is defined as [16]

$$\Delta T_m = T_{cw} - T_m \quad (2)$$

where T_{cw} denotes the temperature from which the dielectric constant starts to deviate from the Curie–Weiss law. For $x=0$, 0.015, 0.03, 0.06 and 0.09, the values of ΔT_m are 197, 209, 213, 236 and 239 °C, respectively, as listed in Table 1. It can be seen that the values of ΔT_m increase with increasing the LN content, which further provides the evidence of composition-induced diffuse phase transition behavior in the $(1-x)$BKT–xLN ceramics with $0 \le x \le 0.09$. As we know, the diffusion phase transition in ABO_3-type perovskite compounds is usually affected by the compositional fluctuation. Because the radius of Li^+ (0.076 nm, CN=12) is smaller than that of Bi^{3+} (0.136 nm, CN=12) and K^+ (0.164 nm, CN=12), and the radius of Ti^{4+} (0.061 nm, CN=6) is close to that of Nb^{5+} (0.064 nm, CN=6) [17], the complex substitution at A-site and B-site tends to cause inhomogeneous composition distribution and disordered crystal structure. Therefore, the enhanced diffuse phase transition in $(1-x)$BKT–xLN solid solutions could be attributed to the multi-ion coexistence at the A-sites and at the B-sites.

For relaxor ferroelectrics with diffuse phase transition, the diffuseness of the phase transition can be more effectively described by a modified Curie–Weiss law [18]

$$1/\varepsilon - 1/\varepsilon_m = (T-T_m)^\gamma / C \quad (3)$$

where γ and C are the diffuseness degree and the Curie constant, respectively. The value of γ varies between 1 (a normal ferroelectric) and 2 (an ideal relaxor ferroelectric). To further confirm the effect of the LN content on the phase transition behavior of $(1-x)$BKT–xLN ceramics, the plots of $\log(1/\varepsilon - 1/\varepsilon_m)$ as a function of $\log(T-T_m)$ at 100 kHz for $(1-x)$BKT–xLN ceramics ($x=0$, 0.03) are shown in Fig. 5. By fitting the experimental data in Fig. 5, the γ values are 1.83 and 1.89 for the $x=0$ and $x=0.03$ samples, respectively. This results indicate that

Table 1
Various parameters of $(1-x)$BKT–xLN ceramics.

x	T_m (°C, 100 kHz)	T_{cw} (°C, 100 kHz)	ΔT_m (°C)	ΔT_{res} (°C)	γ
0	363	560	197	20	1.83
0.015	306	515	209	37	1.85
0.03	294	507	213	46	1.89
0.06	255	491	236	52	1.96
0.09	246	485	239	81	1.99

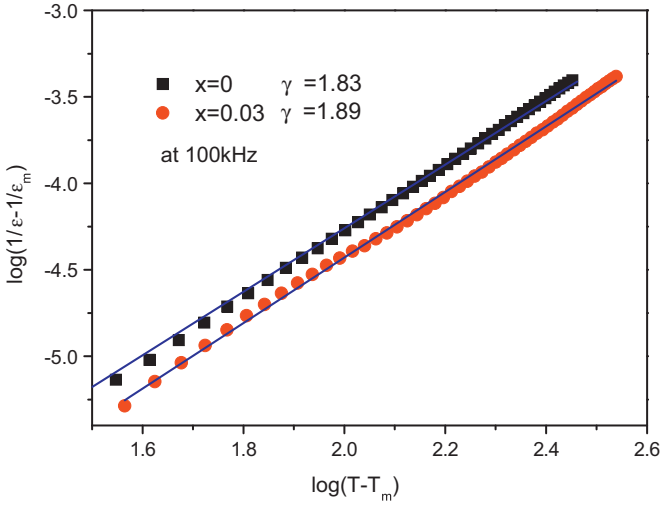

Fig. 5. Plots of $\log(1/\varepsilon-1/\varepsilon_m)$ versus $\log(T-T_m)$ for $(1-x)$BKT–xLN ceramics as indicated.

$(1-x)$BKT–xLN ceramics are typical relaxors. In addition, the relaxor characteristics become more distinct when higher content of LN enters into BKT. Besides the diffuse phase transition, relaxor ferroelectrics also exhibit distinct frequency dispersion of the dielectric constant near and below the phase transition temperature range [19]. The dielectric constant and loss tangents as function of temperature and frequency for the $x=0.015$ sample are shown in Fig. 6. On the one hand, it can be seen that the temperature T_m at the dielectric constant maxima shifts to higher temperatures with increasing frequency. On the other hand, the temperature at the maximum loss tangent also increases with increasing frequency. All these indicate typical frequency dispersion. The parameter ΔT_{res} was often introduced to investigate the empirical relaxation strength by describing the frequency dispersion of T_m, which is defined as [20]

$$\Delta T_{res} = T_{m(1\ \mathrm{MHz})} - T_{m(10\ \mathrm{KHz})} \quad (4)$$

where ΔT_{res} was derived from the dielectric measurements of $(1-x)$BKT–xLN ceramics. The values of ΔT_{res} for all studied samples are also shown in Table 1. These data further confirm that $(1-x)$BKT–xLN ceramics belong to relaxor ferroelectrics.

Fig. 7 shows the electric field-induced polarization hysteresis loops of $(1-x)$BKT–xLN samples. It can be

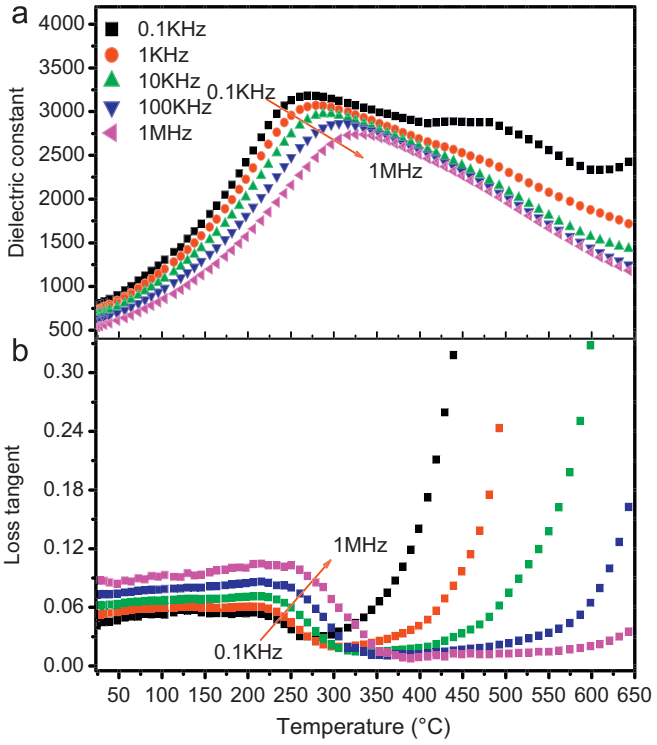

Fig. 6. Dielectric constant (a) and loss tangent (b) of unpoled 0.985BKT–0.015LN ceramics.

seen that typical ferroelectric polarization hysteresis loops were obtained for all samples under an electric field of 60 kV/cm at 10 Hz. The composition dependence of the remanent polarization P_r value and the coercive field E_c is plotted in Fig. 7(b). It is found that the LN content has an effect on the ferroelectric properties of the ceramics. It can be seen that the P_r and E_c values generally decrease with increasing the LN content. However, the P_r value gets slightly increased at $x=0.015$, which might be attributed to the fact that the $x=0.015$ sample lies at the MPB and exhibits the coexistence of two kinds of ferroelectric phases as discussed above. It was generally believed that the coexistence of two kinds of ferroelectric phases makes the domain switching easier under an external electric field. The general tendency of the P_r values also indicates a typical characteristic of the enhanced relaxor behavior with increasing x. The P–E loops looks not very slim probably because of slightly high leakage currents as can

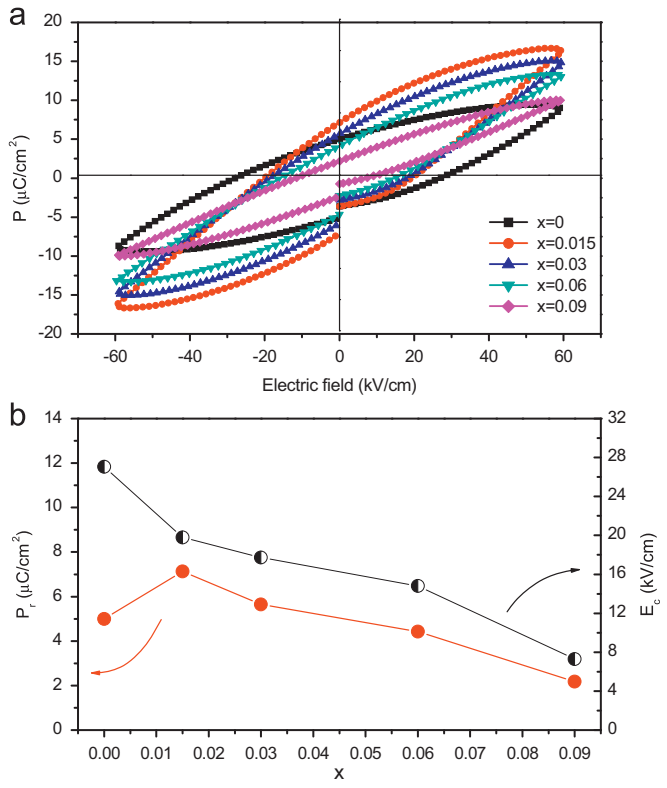

Fig. 7. (a) P–E loops of $(1-x)$BKT–xLN ceramics and (b) the plots of P_r and E_c as a function of the LN content.

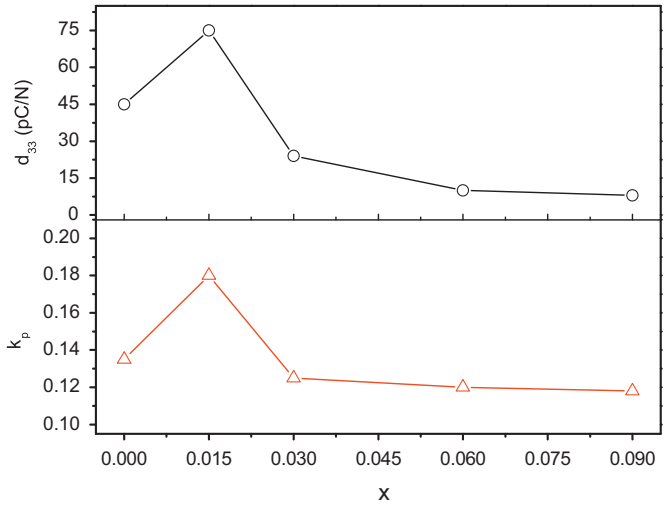

Fig. 8. Piezoelectric and electromechanical properties of poled $(1-x)$BKT–xLN ceramics.

be seen from the round angle of the P–E loops at the maximum electric field.

Fig. 8 shows the piezoelectric coefficient d_{33} and planar coupling factor k_p of $(1-x)$BKT–xLN ceramics as a function of LN content. It can be seen that the piezoelectric properties exhibit obviously compositional dependence because of the existence of the phase transition between rhombohedral and tetragonal ferroelectric phases. The best piezoelectric properties of $d_{33}\sim 75$ pC/N and $k_p\sim 0.18$ appear in the composition with $x=0.015$, which is located near MPB. This phenomenon is similar to that observed in conventional Pb-based piezoelectric ceramics. The coexistence of two ferroelectric phases provides more spontaneous polarization directions, leading to higher piezoelectric activity. Nevertheless, the piezoelectric properties of this system are not high enough for industrial application. In order to enhance the electrical properties, some donor dopants such as Nb^{5+} can be used in the future work.

4. Conclusions

The $(1-x)$BKT–xLN solid solution ceramics have been prepared by a mixed oxide route and an ordinary sintering technique. The XRD patterns indicate that single perovskite structure has formed in specimens with $x<0.09$ and an MPB was identified to be in the range of $0.015<x<0.03$. With increasing the LN content, the strongly frequency-dependent dielectric constant peak at T_m shifts to lower temperatures and becomes broader, indicating that the addition of LN tends to enhance the relaxor behavior probably induced by an increase of the disorder at A and B sites. The optimum electrical properties of $d_{33}=75$ pC/N, $k_p=0.18$, $P_r=7.1$ μC/cm^2, $E_c=19.8$ kV/cm and $T_c=306$ °C were achieved in $(1-x)$BKT–xLN ceramics with $x=0.015$, owing to the coexistence of two kinds of ferroelectric phases near MPB.

Acknowledgments

This work was financially supported by a project of Natural Science Foundation of Anhui Province (1108085J14), the National Natural Science Foundation of China (50972035), and a Program for New Century Excellent Talents in University, State Education Ministry (NCET-08-0766).

References

[1] Y. Saito, H. Takao, T. Tani, T. Nonoyama, K. Takatori, T. Homma, T. Nagaya, Lead-free piezoceramics, Nature 432 (2004) 84–87.
[2] B.P. Zhang, J.F. Li, K. Wang, H.L. Zhang, Compositional dependence of piezoelectric properties in $Na_xK_{1-x}NbO_3$ lead-free ceramics prepared by Spark plasma sintering, Journal of the American Ceramic Society 89 (2006) 1065–1609.
[3] R.Z. Zuo, Y. Liu, S. Su, X.C. Chu, X.H. Wang, Phase transformation behavior and electrical properties of $Pb(Zr_{0.56}Ti_{0.44})O_3$–$Bi(Zn_{0.5}Ti_{0.5})O_3$ solid solution ceramics, Journal of the American Ceramic Society 94 (2011) 4340–4344.
[4] Y. Hiruma, R. Aoyagi, H. Nagata, T. Takenaka, Ferroelectric and piezoelectric properties of $(Bi_{1/2}K_{1/2})TiO_3$ ceramics, Japanese Journal of Applied Physics 44 (2005) 5040–5044.
[5] S.G. Jun, N.K. Kim, Dielectric properties of PFW–PMN relaxor system prepared by B-site precursor method, Journal of Materials Science 35 (2000) 2093–2097.
[6] M. Ahart, H. Mao, R.E. Cohen, R.J. Hemley, Pressure effects on relaxor ferroelectricity in disordered $Pb(Sc_{1/2}Nb_{1/2})O_3$, Journal of Applied Physics 107 (2010) 074110-074110-5.

[7] A. Mesquita, V.R. Mastelaro, A. Michalowicz, In-situ X-ray diffraction studies of phase transition in $Pb_{1-x}La_xZr_{0.40}Ti_{0.60}O_3$ ferroelectric ceramics, Phase Transitions 83 (2010) 251–262.

[8] Y. Ishii, K. Nomura, F. Fukuda, H. Asada, T. Aihara, B-ion substitution in (Pb–A)(Ti–B)O_3 systems with A=$Na_{1/2}Bi_{1/2}$ or $K_{1/2}Bi_{1/2}$ and B=Zr, $Fe_{1/2}Nb_{1/2}$, $Zn_{1/3}Nb_{2/3}$, $Mg_{1/3}Nb_{2/3}$ or $Mg_{1/2}W_{1/2}$, Japanese Journal of Applied Physics 34 (1995) 4849–4853.

[9] R.Z. Zuo, X.S. Fang, C. Ye, L.T. Li, Phase transitional behavior and piezoelectric properties of lead-free $(Na_{0.5}K_{0.5})NbO_3$–$(Bi_{0.5}K_{0.5})TiO_3$ ceramics, Journal of the American Ceramic Society 90 (2007) 2424–2428.

[10] H. Matsuo, Y. Noguchi, M. Miyayama, M. Suzuki, M.A. Watanabe, Structural and piezoelectric properties of high-density $(Bi_{0.5}K_{0.5})$-TiO_3–$BiFeO_3$ ceramics, Journal of Applied Physics 108 (2010) 104103-104103-6.

[11] I. Inbar, R.E. Cohen, Origin of ferroelectricity in $LiNbO_3$ and $LiTaO_3$, Ferroelectrics 194 (1997) 83–95.

[12] K. Kakimoto, K. Akao, K.Y.P. Guo, H. Ohsato, Raman scattering study of piezoelectric $(Na_{0.5}K_{0.5})NbO_3$–$LiNbO_3$ ceramics, Japanese Journal of Applied Physics 44 (2005) 7064–7067.

[13] J.S. Kim, C.H. Chung, H.S. Lee, Dielectric and ferroelectric properties of $LiNbO_3$ doped lead-free $Bi_{0.5}Na_{0.5}TiO_3$ (BNT) ceramics, Journal of the Korean Physical Society 58 (2011) 659–662.

[14] C.R. Zhou, X.Y. Liu, W.Z. Li, C.L. Yuan, Microstructure and electrical properties of $Bi_{0.5}Na_{0.5}TiO_3$–$Bi_{0.5}K_{0.5}TiO_3$–$LiNbO_3$ lead-free piezoelectric ceramics, Journal of Physics and Chemistry of Solids 70 (2009) 541–545.

[15] M. Otonicar, S.D. Skapin, B. Jancar, R. Ubic, D. Suvorov, Analysis of the phase transition and the domain structure in $K_{0.5}Bi_{0.5}TiO_3$ perovskite ceramics by in situ XRD and TEM, Journal of the American Ceramic Society 93 (2010) 4168–4173.

[16] X.G. Tang, X.X. Wang, K. Chew, H.L.W. Chan, Relaxor behavior of (Ba, Sr)(Zr, Ti)O_3 ferroelectric ceramics, Solid State Communications 136 (2005) 89–93.

[17] R.D. Shannon, Revised effective ionic radii and systematic studies of interatomie distances in halides and chaleogenides, Acta Crystallographica Section A 32 (1976) 751–767.

[18] K. Uchino, S. Nomura, Critical exponents of the dielectric constants in diffused-phase-transition crystals, Ferroelectrics 44 (1982) 55–61.

[19] V.V. Shvartsman, D.C. Lupascu, Lead-free relaxor ferroelectrics, Journal of the American Ceramic Society 95 (2012) 1–26.

[20] T. Badapanda, S.K. Rout, S. Panigrahi, T.P. Sinha, Relaxor behaviour of $(Ba_{0.5}Sr_{0.5})(Ti_{0.6}Zr_{0.4})O_3$ ceramics, Bulletin of Materials Science 31 (2008) 897–901.